

# **Ti<sub>2</sub>S@D<sub>3h</sub>(24109)-C<sub>78</sub>: A sulfide cluster metallofullerene containing only non-rare earth metals inside the cage**

Fang-Fang Li,<sup>a</sup> Ning Chen,<sup>a,c</sup> Marc Mulet-Gas,<sup>b</sup> Vivian Triana,<sup>a</sup> Jesse Murillo,<sup>a</sup> Antonio Rodríguez-Forteza,<sup>\*b</sup> Josep M. Poblet,<sup>\*b</sup> and Luis Echegoyen<sup>\*a</sup>

<sup>a</sup> Department of Chemistry, University of Texas at El Paso, El Paso, Texas 79968, United States

<sup>b</sup> Departament de Química Física i Inorgànica, Universitat Rovira i Virgili, 43007 Tarragona, Spain

<sup>c</sup> Current address: College of Chemistry, Chemical Engineering and Materials Science, Soochow University, Suzhou, Jiangsu, 212163, China. Email: chenning@suda.edu.cn

Email: antonio.rodriguez@urv.cat, josepmaria.poblet@urv.cat, echegoyen@utep.edu

## **Abstract**

A new titanium-based sulfide clusterfullerene, Ti<sub>2</sub>S@D<sub>3h</sub>(24109)-C<sub>78</sub>, has been successfully synthesized by arc-discharging graphite rods packed with pure TiO<sub>2</sub> and graphite powder under an atmosphere of SO<sub>2</sub> and helium. Multistage HPLC methods were utilized to isolate and purify the Ti<sub>2</sub>S@C<sub>78</sub>, and mass spectrometric characterization confirmed the composition of a Ti<sub>2</sub>S cluster within a C<sub>78</sub> cage. UV-Vis-NIR absorption spectroscopy, electrochemical characterization and extensive DFT calculations led to the assignment of the cage symmetry to D<sub>3h</sub>(24109)-C<sub>78</sub> and suggested an almost linear arrangement of the internal Ti<sub>2</sub>S cluster, with a formal transfer of six electrons from the cluster to the C<sub>78</sub> cage.

## **Introduction**

Endohedral metallofullerenes (EMFs) are continuously attracting attention from scientists due to (i) the variable structures induced by combining different encaged clusters with different size/symmetry carbon cages;<sup>1-4</sup> (ii) the interesting electronic properties resulting from charge transfer from the encapsulated moiety to the carbon shell;<sup>1</sup> and (iii) the potential applications of both pristine and functionalized EMFs.<sup>1,5-11</sup> A substantial amount of experimental and theoretical effort has been devoted to studies of EMFs.<sup>12-17</sup>

The cluster metallofullerenes are a special class of EMFs. Since the discovery of the first cluster fullerene, Sc<sub>3</sub>N@C<sub>80</sub>, with a Sc<sub>3</sub>N cluster inside a C<sub>80</sub> cage in 1999,<sup>18</sup> the horizons of this field have been expanded considerably and a new era in the field of EMFs began. Up until now, the types of cluster metallofullerenes reported are nitride

cluster metallofullerenes (NCFs,  $M_3N@C_{2n}$ ),<sup>1,3,4,18,19</sup> carbide cluster metallofullerenes (CCFs,  $M_{2-4}C_2@C_{2n}$ ),<sup>1,3,20-24</sup> oxide cluster metallofullerenes (OCFs,  $M_xO_y@C_{2n}$   $x = 2-4$ ,  $y = 1-3$ ),<sup>1,3,25-27</sup> carbonitride cluster metallofullerenes (CNCFs,  $M_3NC@C_{2n}$ ),<sup>3,28,29</sup> hydrocarbide cluster metallofullerenes (HCCFs,  $M_3CH@C_{2n}$ )<sup>3,30</sup> and sulfide cluster metallofullerenes (SCFs,  $M_2S@C_{2n}$ ).<sup>31-36</sup> SCFs are the most recently developed cluster fullerene family and only a few, such as  $M_2S@C_{82}$  ( $M = Sc, Y, Lu, Dy$ )<sup>31</sup> and  $Sc_2S@C_{2n}$  ( $n = 35, 36, 41$ ),<sup>32-34</sup> have been isolated and reported. These new fullerenes have yet to be fully explored. Much is still to be discovered by using other metals in the SCFs synthesis.

All of the reported cluster fullerenes contain encapsulated rare earth metals *i.e.* group-III (Sc, Y, and lanthanides), and there are very few reports of cluster fullerenes with a non-rare earth metal trapped inside the carbon cage. In 1992, encaging of only non-rare earth metals inside a carbon cage was reported,  $Ti@C_{28}$ , which was only observed by mass spectrometry.<sup>37,38</sup> In 2001, a titanium carbide cluster fullerene,  $Ti_2@C_{80}$ ,<sup>39</sup> whose structure was later determined to be  $Ti_2C_2@D_{3h}-C_{78}$ ,<sup>40-42</sup> and  $Ti_2@C_{84}$ <sup>43</sup> were isolated and identified. In 2009, Yang and coworkers attempted to synthesize Ti-only nitride cluster fullerenes using pure  $TiO_2$ , however, no Ti-containing NCFs were detected in the extract. Subsequently, they modified the method using a  $TiO_2/Sc_2O_3$  mixture instead of pure  $TiO_2$  and achieved the first mixed metallic nitride cluster fullerene encapsulating Ti,  $TiSc_2N@I_h-C_{80}$ .<sup>44</sup> Following the same synthetic procedure using a  $TiO_2/Y_2O_3$  mixture,  $TiY_2N@I_h-C_{80}$  was synthesized.<sup>45</sup> On the basis of these results, the synthesis of Ti only NCFs seems impractical using just  $TiO_2$ , it must be accompanied by rare earth metals such as Sc and Y, and only one Ti atom seems to be encaged. An alternative way to encage a Ti-only cluster could involve the use of a sulfide instead of nitride in this work, thus we used  $SO_2$  instead of  $N_2$  as a gas source. Here we report the first sulfide clusterfullerene with no rare-earth metals inside the cage,  $Ti_2S@C_{78}$ , where the cage has  $D_{3h}(24109)-C_{78}$  symmetry and the  $Ti_2S$  cluster is almost perfectly linear.

## Results and discussion

### Synthesis and isolation of $Ti_2S@C_{78}$

$Ti_2S@C_{78}$  was synthesized in a conventional Krätschmer–Huffman reactor using a  $TiO_2$ /graphite powder mixture in a weight ratio of 1:4 in a mixture of helium (200 torr)

and SO<sub>2</sub> (20 torr) atmosphere. The procedures are very similar to those already described for the synthesis of Sc sulfide cluster fullerenes.<sup>32</sup> The as-produced soot was pre-extracted with ether and further extracted with CS<sub>2</sub> for 4 hours and analyzed by HPLC and MALDI-TOF-MS (matrix-assisted laser desorption ionization time-of-flight mass spectrometry). Figure 1 shows the initial HPLC of the extract. The MALDI-TOF MS analysis shows that the Ti<sub>2</sub>S@C<sub>78</sub> fraction is overlapped with those of C<sub>88</sub>, C<sub>90</sub>, C<sub>92</sub> and Ti<sub>2</sub>@C<sub>84</sub> as shown in Figure 1. Multistage HPLC methods were utilized to isolate and purify the Ti<sub>2</sub>S@C<sub>78</sub> (see Figure S1 in ESI). The purity of Ti<sub>2</sub>S@C<sub>78</sub> was established using HPLC as an inset in Figure 1.

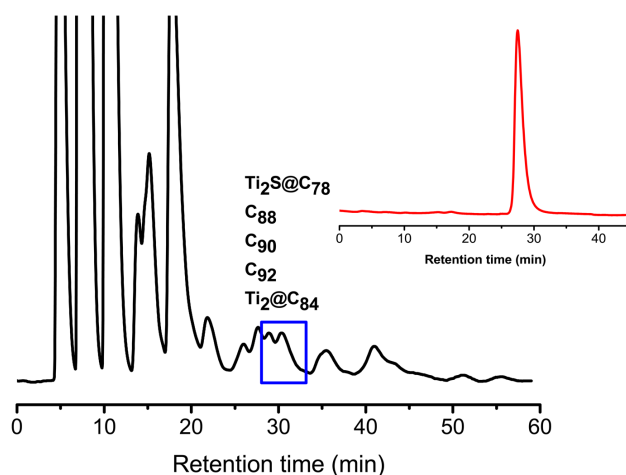


**Fig. 1** HPLC chromatogram from the initial extract on a 5PYE column. Inset: HPLC of the purified Ti<sub>2</sub>S@C<sub>78</sub> on a Buckyprep-M column. Conditions:  $\lambda = 320$  nm; mobile phase, toluene; flow rate, 4.00 mL/min.

### **Spectroscopic structure determination of Ti<sub>2</sub>S@C<sub>78</sub>**

The purified Ti<sub>2</sub>S@C<sub>78</sub> was initially characterized by mass spectrometry. The MALDI-TOF mass spectrum, shown in Figure 2, shows a single peak with  $m/z$  at 1063.866, corresponding to the mass of Ti<sub>2</sub>S@C<sub>78</sub>, which also suggests that the sample is reasonably pure. The inset shows the simulated and experimental mass spectra of Ti<sub>2</sub>S@C<sub>78</sub>. The experimental isotopic distribution of Ti<sub>2</sub>S@C<sub>78</sub> shows excellent agreement with the theoretical one, further corroborating the composition of Ti<sub>2</sub>S@C<sub>78</sub>. Two titanium atoms are successfully stabilized within a fullerene cage in the form of a sulfide cluster. However, we did not observe an extensive family for Ti<sub>2</sub>S cluster

fullerenes as in the case of sulfide cluster fullerenes ( $\text{Sc}_2\text{S}@C_{2n}$  ( $n = 35-50$ )),<sup>32</sup> which indicates once again the difficulties of trapping non-rare earth metals inside the carbon cages.

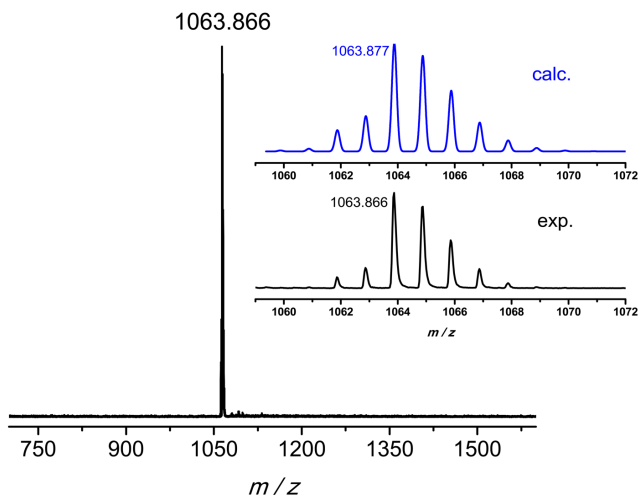


**Fig. 2** MALDI-TOF mass spectrum of the HPLC-purified  $\text{Ti}_2\text{S}@C_{78}$ . The inset shows the simulated and experimental isotopic distributions for the corresponding  $\text{Ti}_2\text{S}@C_{78}$ .

The  $C_{78}$  cage can exist in 24109 isomeric forms, with five that obey the isolated pentagon rule (IPR) [ $D_3(78: 24105)$ ,  $C_{2v}(78: 24106)$ ,  $C_{2v}(78: 24107)$ ,  $D_{3h}(78: 24108)$ , and  $D_{3h}(78: 24109)$ ].<sup>46</sup> In order to help assign the cage isomer, the UV-Vis-NIR spectroscopy was recorded. Shinohara showed that similar UV-Vis-NIR spectra are indicative of EMFs possessing the same cage structures.<sup>47</sup> Popov and Dunsch also reported that similar electronic spectral features indicate the same cage geometry since the electronic absorptions of fullerenes are predominantly due to  $\pi-\pi^*$  carbon cage transitions.<sup>2,4,15</sup> Therefore, UV-Vis-NIR spectroscopy has been extensively used to predict fullerene cage geometries and to probe the electronic structures of endohedral metallofullerenes. Figure 3 shows the UV-Vis-NIR absorption spectrum of  $\text{Ti}_2\text{S}@C_{78}$ . Absorptions at 498, 602, 657, 757 and 896 nm were observed with an onset around 1470 nm, indicating that this titanium sulfide cluster fullerene possesses a small HOMO-LUMO gap. The optical band-gap of  $\text{Ti}_2\text{S}@C_{78}$  is estimated to be 0.84 eV based on the absorption spectral onset which is smaller than that of  $\text{Ti}_2\text{C}_2@C_{78}$ .<sup>39</sup> The feature-rich absorptions of  $\text{Ti}_2\text{S}@C_{78}$  resemble those of  $\text{Ti}_2\text{C}_2@D_{3h}\text{-}C_{78}$ <sup>39</sup> and  $\text{Sc}_3\text{N}@D_{3h}(24109)\text{-}$

$C_{78}$ <sup>48,49</sup> and are dramatically different from that of  $M_3N@C_2-C_{78}$  ( $M = Gd, Sc, Tm, Dy$ ).<sup>29,49,50</sup> In addition,  $Ti_2S@C_{78}$  displays the same green color in toluene/ $CS_2$  as  $Sc_3N@D_{3h}(24109)-C_{78}$  does, which strongly suggests that the geometric and electronic structure of  $Ti_2S@C_{78}$  are similar to those of  $Sc_3N@D_{3h}(24109)-C_{78}$ .<sup>48,49</sup> Based on these observations we assign the  $D_{3h}(24109)$  cage symmetry to  $Ti_2S@C_{78}$ , which was also confirmed by theoretical calculations, see below. Multiple attempts to obtain suitable crystal for X-ray diffraction analysis were not successful.  $Sc_3N@D_{3h}(24109)-C_{78}$  formally undergoes a six-electron transfer from the cluster to the cage.<sup>51</sup> Assuming that a six-electron transfer is present in  $Ti_2S@C_{78}$ , the oxidation state of titanium is  $Ti^{4+}$ , not  $Ti^{3+}$ , as is the case for  $Sc_2TiN@C_{80}$ <sup>44</sup> and  $Y_2TiN@C_{80}$ .<sup>45</sup> Thus according to the ionic model,<sup>51,52</sup>  $Ti_2S@C_{78}$  can be formally considered to be  $(Ti_2S)^{6+}@D_{3h}(24109)-C_{78}^{6-}$ .

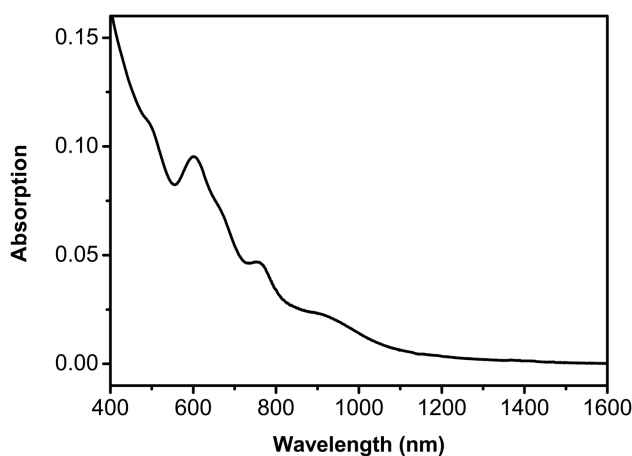


**Fig. 3** UV-Vis-NIR spectrum of  $Ti_2S@C_{78}$  in toluene.

### Electrochemistry studies

Cyclic voltammetry (CV) is the most common technique used to explore the electrochemical behavior of EMFs. The CV of  $Ti_2S@C_{78}$  in an *o*-dichlorobenzene (*o*-DCB) solution containing 0.05 M tetra-*n*-butylammonium hexafluorophosphate (*n*-Bu<sub>4</sub>NPF<sub>6</sub>) as the supporting electrolyte is displayed in Figure 4. Using a scan rate of 100 mV/s,  $Ti_2S@C_{78}$  exhibits three reversible reductions with half wave potentials at  $-0.92$ ,  $-1.53$ , and  $-1.80$  V, respectively, versus  $Fc/Fc^+$  and two additional irreversible reductions with peak potentials at  $-2.29$  and  $-2.41$  V, respectively. In the anodic scan, two

reversible oxidation steps with half wave potentials at +0.23 and +0.65 V are observed, along with one quasi-reversible oxidation at +1.03 V versus Fc/Fc<sup>+</sup>.

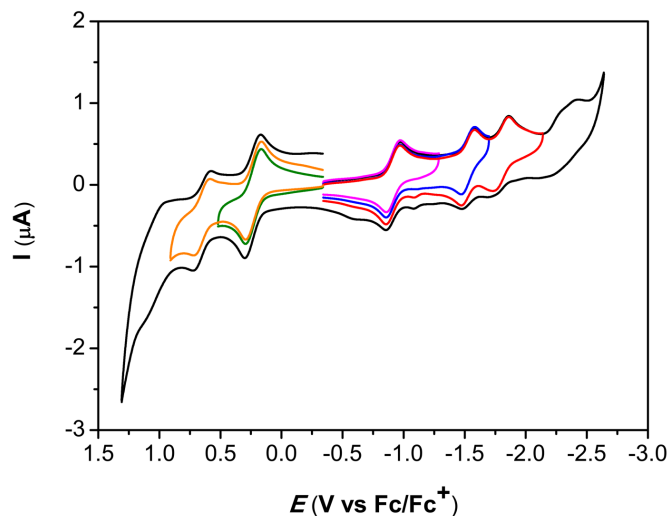


**Fig. 4** Cyclic voltammogram of Ti<sub>2</sub>S@C<sub>78</sub> recorded in a 0.05 M *o*-DCB/*n*-Bu<sub>4</sub>NPF<sub>6</sub> solution at a scan rate of 100 mV/s. Ferrocene (Fc) was added as the internal standard.

The electrochemically reversible behavior of Ti<sub>2</sub>S@D<sub>3h</sub>-C<sub>78</sub> is dramatically different from those of most metallic cluster fullerenes which usually display irreversible reductions under the same conditions.<sup>1</sup> TiSc<sub>2</sub>N@C<sub>80</sub>,<sup>44,53</sup> Sc<sub>2</sub>S@C<sub>72</sub><sup>33</sup> and Sc<sub>4</sub>O<sub>2</sub>@C<sub>80</sub><sup>54</sup> are some of the very few clusterfullerenes with cages ≤ C<sub>80</sub> that exhibit reversible reductions. Although Sc<sub>3</sub>N@D<sub>3h</sub>-C<sub>78</sub> presumably possesses the same cage isomer as Ti<sub>2</sub>S@D<sub>3h</sub>-C<sub>78</sub> does, the CV of Sc<sub>3</sub>N@D<sub>3h</sub>-C<sub>78</sub> shows irreversible reduction steps,<sup>1,55</sup> which indicates that the encaged clusters have a significant influence on the electrochemical behavior. Moreover, the first reduction and the first oxidation potentials of Ti<sub>2</sub>S@D<sub>3h</sub>-C<sub>78</sub> are anodically shifted by 620 mV and 110 mV, respectively, compared with those of Sc<sub>3</sub>N@D<sub>3h</sub>-C<sub>78</sub>. Hence, Ti<sub>2</sub>S@D<sub>3h</sub>-C<sub>78</sub> is much easier to reduce and somewhat harder to oxidize than Sc<sub>3</sub>N@D<sub>3h</sub>-C<sub>78</sub>. The electrochemical gap of Ti<sub>2</sub>S@D<sub>3h</sub>-C<sub>78</sub>, 1.15 V, is 0.51 V less than that of Sc<sub>3</sub>N@D<sub>3h</sub>-C<sub>78</sub> (1.66 V) (Table 1) and is comparable to that of TiSc<sub>2</sub>N@I<sub>h</sub>-C<sub>80</sub> (1.10 V)<sup>44</sup> (Table 1), which is 0.75/0.76 V less than that of Sc<sub>3</sub>N@I<sub>h</sub>-C<sub>80</sub> (1.85<sup>56</sup>/1.86 V<sup>57</sup>). Similarly, TiY<sub>2</sub>N@I<sub>h</sub>-C<sub>80</sub> has an electrochemical gap of 1.11 V<sup>45</sup> (Table 1), which is 0.94 V less than that of the corresponding Y<sub>3</sub>N@C<sub>80</sub> (2.05 V).<sup>1,45,58</sup> The electrochemical gap of Ti<sub>2</sub>S@D<sub>3h</sub>-C<sub>78</sub> is also 0.22-0.63 V less than

those of the reported Sc<sub>2</sub>S cluster fullerenes. These results confirm that Ti-containing cluster fullerenes possess smaller electrochemical gaps than the corresponding rare earth metallic cluster fullerenes. Interestingly, the electrochemical and low temperature ESR measurements of TiSc<sub>2</sub>N@C<sub>80</sub> conducted by Popov and Dunsch<sup>53</sup> have shown that the unpaired electron in TiSc<sub>2</sub>N@C<sub>80</sub> is mainly localized on the Ti ion, thus the endohedral TiSc<sub>2</sub>N cluster is the electrochemically active species. Both reduction and oxidation occurred at the TiSc<sub>2</sub>N cluster. The results have clearly shown that the redox chemistry of Ti-containing mixed-metal nitride EMFs is controlled by the Ti atom.

**Table 1** Redox potentials (V vs Fc/Fc<sup>+</sup>) of Ti<sub>2</sub>S@D<sub>3h</sub>-C<sub>78</sub> along with other related cluster fullerenes.

Compounds	$E^{+/2+}$ [V]	$E^{0/+}$ [V]	$E^{0/}$ [V]	$E^{-/}$ [V]	$E^{2-/}$ [V]	$\Delta E_{gap,ec}$ [V]
Ti <sub>2</sub> S@D <sub>3h</sub> -C <sub>78</sub>	+0.65 <sup>a</sup>	+0.23 <sup>a</sup>	-0.92 <sup>a</sup>	-1.53 <sup>a</sup>	-1.80 <sup>a</sup>	1.15
Sc <sub>3</sub> N@D <sub>3h</sub> -C <sub>78</sub> <sup>55</sup>		+0.12 <sup>a</sup>	-1.54 <sup>b</sup>			1.66
TiSc <sub>2</sub> N@I <sub>h</sub> -C <sub>80</sub> <sup>44</sup>		+0.16 <sup>a</sup>	-0.94 <sup>a</sup>	-1.58 <sup>a</sup>	-2.21 <sup>a</sup>	1.10
TiY <sub>2</sub> N@I <sub>h</sub> -C <sub>80</sub> <sup>45</sup>		+0.00 <sup>a</sup>	-1.11 <sup>a</sup>	-1.79 <sup>b</sup>		1.11

<sup>a</sup>Half-wave potential. <sup>b</sup>Peak potential.

### Computational studies

An extensive computational analysis was conducted to confirm the symmetry of the C<sub>78</sub> cage that is encapsulating the Ti<sub>2</sub>S cluster. For the C<sub>78</sub> family, there are a total of 24109 cage isomers. Among them, we considered all the structures that (i) satisfy the isolated pentagon rule (IPR, 5 isomers); (ii) show one adjacent pentagon pair (APP1, 18 isomers); and (iii) show two pairs of adjacent pentagons (APP2, 228 isomers). The adjacent pentagons, also called pentalene units, are seen to interact with the metal ions of the cluster, thus providing an extra stabilization via both ionic and covalent contributions.<sup>59-62</sup> No structures with three or more APPs were considered because they are found at much higher energies and there are only two Ti ions in the cluster able to interact with up to two pentalene units. From the electronic structure of the lowest-energy clusterfullerenes analyzed, we confirmed that there is a formal transfer of six electrons from the Ti<sub>2</sub>S cluster to the C<sub>78</sub> cage, (Ti<sub>2</sub>S)<sup>6+</sup>@C<sub>78</sub><sup>6-</sup>, as proposed from the experimental UV-Vis-NIR spectrum (see orbital interaction diagram, Figure 5). We first computed at the AM1 level

the hexaanions for the 251 cages with less than three APPs and then, the lowest-energy hexaanions and the corresponding clusterfullerenes at the DFT level (see Table 2). A correlation between the relative energies of the clusterfullerenes and those of the hexaanions was observed, further confirmation of the validity of the ionic model (see Figure S2 in ESI).

The clusterfullerene with the  $D_{3h}$ - $C_{78}(24109)$  cage was found to be, by a large difference, the one with the lowest energy, see Table 2. This IPR cage shows the maximal separation between pentagons, in good agreement with the rule established by Poblet and co-workers.<sup>ref60</sup> Other isomers were found to have more than 20 kcal mol<sup>-1</sup> higher energies (Table 2). Interestingly, the relative energies of clusterfullerenes with respect to  $Ti_2S@D_{3h}-C_{78}(24109)$  were larger than those computed for the hexaanions. This indicates that there is an extra stabilization of the system due to the favorable interaction between the  $Ti_2S$  cluster and the  $D_{3h}$ - $C_{78}(24109)$  cage, for which the Ti–S and Ti•••C distances are optimal. In fact, the different orientations of the  $Ti_2S$  cluster inside the  $D_{3h}$ - $C_{78}(24109)$  cage show significant energy differences (up to 30 kcal mol<sup>-1</sup>, see Table S1 in ESI), the most favorable being the one with the cluster in an almost collinear position (Ti–S–Ti angle of 172 degrees) with the  $C_3$  axis of the  $D_{3h}$ - $C_{78}(24109)$  cage, as shown in Figure 6. For all cluster fullerenes possessing non-IPR cages, the most favorable orientations of the internal cluster are those in which the Ti atoms are interacting with the pentalene units (see Figure 6). Therefore, for a given cage, the structure of the  $Ti_2S$  cluster adapts in order to (i) optimize the interaction with the fullerene, for example Ti ions pointing to the pentalene units for non-IPR cages; and (ii) minimize the repulsion between formal  $Ti^{4+}$  cations, *i.e.* by assuming a linear Ti–S–Ti arrangement. Cage  $D_{3h}$ - $C_{78}(24109)$  satisfies the three required conditions to host the  $Ti_2S$  cluster: (i) It is the most suitable isomer to accept the six electron transfer; (ii) It shows optimal Ti•••C interactions; and (iii) It allows the internal cluster to be in an almost linear arrangement with maximally separated  $Ti^{4+}$  ions.

**Table 2** Relative energies (in kcal mol<sup>-1</sup>) for several isomers of  $C_{78}$  in the hexaanion and endohedral forms.<sup>a,b</sup>

Isomer	Symmetry	APP	$C_{78}^{6-}$	$Ti_2S@C_{78}$
--------	----------	-----	---------------	----------------

21828	$C_1$	2	43.6	68.1
21975	$C_1$	2	29.8	44.0
21981	$C_1$	2	31.7	49.9
21982	$C_1$	2	36.3	54.6
21983	$C_1$	2	54.4	42.0
22010	$C_2$	2	15.4	29.2
22033	$C_1$	2	57.2	72.8
22096	$C_1$	2	52.2	59.6
22135	$C_1$	2	36.1	50.5
22590	$C_1$	2	42.5	51.5
22646	$C_1$	2	27.3	41.5
23298	$C_2$	2	39.9	60.1
23349	$C_1$	1	32.2	38.7
24088	$C_{2v}$	2	28.4	23.6
24101	$C_s$	2	65.8	49.5
24105	$D_3$	0	48.1	78.5
24106	$C_{2v}$	0	57.0	63.0
24107	$C_{2v}$	0	23.7	31.6
24108	$D_{3h}$	0	79.3	104.0
24109	$D_{3h}$	0	0.0	0.0

<sup>a</sup> Isomer number according to the spiral algorithm of Fowler and Manolopoulos.<sup>46</sup> <sup>b</sup> APP: number of adjacent pentagon pairs.

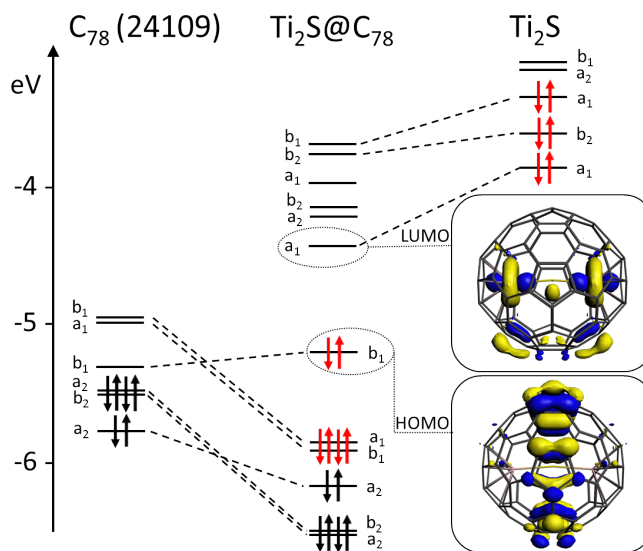


**Fig. 5** Orbital interaction diagram for  $Ti_2S@D_{3h}-C_{78}(24109)$ . The fragments,  $Ti_2S$  and  $D_{3h}-C_{78}(24109)$ , were calculated with the same geometry that they have in the clusterfullerene. Six electrons from the neutral  $Ti_2S$  cluster (those represented by red arrows) are formally transferred to cage orbitals.

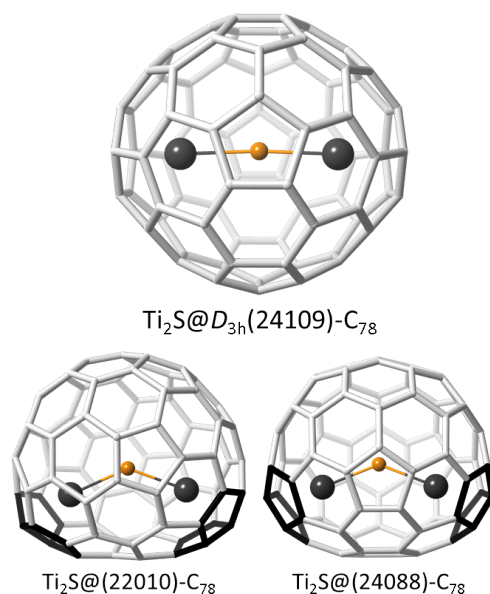


**Fig. 6** DFT-optimized structures for the lowest-energy IPR and APP2  $\text{Ti}_2\text{S}@C_{78}$  clusterfullerenes.

The orbital interaction diagram for the lowest-energy clusterfullerene  $\text{Ti}_2\text{S}@D_{3h}\text{-C}_{78}(24109)$ , see Figure 5, verifies that there is a formal transfer of six electrons from the cluster to the cage,  $(\text{Ti}_2\text{S})^{6+}@C_{78}^{6-}$ , as also seen for nitride  $\text{Sc}_3\text{N}@D_{3h}\text{-C}_{78}(24109)$  and carbide  $\text{Ti}_2\text{C}_2@d_{3h}\text{-C}_{78}(24109)$ . The HOMO is mainly localized on the fullerene. The LUMO, however, has predominant contributions from the  $\text{Ti}_2\text{S}$  cluster; in particular, from the bonding combination of the  $d_{z^2}$ -like atomic orbitals of the two Ti ions (Figure 5). The computed HOMO-LUMO gap for  $\text{Ti}_2\text{S}@D_{3h}\text{-C}_{78}(24109)$ , 0.66 eV, is significantly smaller than the gap for the hexaanionic cage, 1.22 eV. This small HOMO-LUMO gap is in good agreement with the experimental results that show small optical and electrochemical gaps. It is worth remarking here that, given the topology of the frontier orbitals, the oxidation of the clusterfullerene is predicted to take place on the carbon cage. The reduction is, however, predicted to happen in *cavea*, *i.e.* in the internal cluster, as in  $\text{M}_2@C_{80}$  ( $\text{M} = \text{La}, \text{Ce}$ )<sup>63,64</sup> or  $\text{TiM}_2\text{N}@C_{80}$  ( $\text{M} = \text{Sc}, \text{Y}$ ).<sup>44,45</sup> Since the formal oxidation state of Ti is +4 in  $\text{Ti}_2\text{S}@C_{78}$ , the oxidation process of the endohedral cannot be based on the Ti centers, so the Ti atoms control only the reduction processes in this case, in contrast with the redox results reported by Popov and Dunsch for  $\text{TiSc}_2\text{N}@C_{80}$ , where the  $\text{Ti}^{3+}$  centers are responsible for both the reductive and oxidative electrochemical

behavior.<sup>53</sup> Computed oxidation and reduction potentials agree reasonably well with the experimental values measured by cyclic voltammetry. The first anodic potential is predicted at +0.08 V, in rather good agreement with the measured half-wave potential, +0.23 V (Table 3). The predicted first cathodic potential, -1.02 V, is also close to the experimental value with a difference of only 100 mV (Table 3). Computation of the spin density for the singly reduced  $\text{Ti}_2\text{S}@D_{3h}\text{-C}_{78}^-$  confirms that reduction takes place in the internal cluster (see Figure S3 in ESI). The computed electrochemical (EC) gap, 1.10 V, also compares very well with the experimental value, 1.15 V. We have been able to compute the second oxidation potential, at 0.56 V, which is within less than 100 mV from the experimental value (Table 3).

**Table 3** Experimental and computed oxidation and reduction potentials (in V versus  $\text{Fc}^+/\text{Fc}$ ), as well as the computed HOMO-LUMO gap (in eV) for  $\text{Ti}_2\text{S}@D_{3h}\text{-C}_{78}$ .

	$E^{+/2+}$	$E^{0/+}$	$E^{0/-}$	$\Delta E_{\text{gap},ec}$	$H-L_{\text{gap}}$
Experimental	+0.65	+0.23	-0.92	1.15	
Computed	+0.56	+0.08	-1.02	1.10	0.66

The molar fractions of the lowest-energy  $\text{Ti}_2\text{S}@C_{78}$  isomers as a function of the temperature were also computed using the rigid rotor and harmonic oscillator (RRHO) approximation and the related free-encapsulating model (FEM) as proposed by Slanina.<sup>65,66</sup> The two approximations provide the same predictions, *i.e.*  $\text{Ti}_2\text{S}@D_{3h}\text{-C}_{78}(24109)$  is the most abundant isomer for the whole temperature range up to 4000 K (see Figure S4 in ESI). Acceptable agreement is also observed with the experimental UV-Vis-NIR spectrum. We have computed it for  $\text{Ti}_2\text{S}@D_{3h}\text{-C}_{78}(24109)$  using time-dependent (TD) DFT in the Vis-NIR region, for wavelengths larger than 450 nm. Despite the systematic underestimation of excitation energies by TD-DFT, this methodology provides reasonable agreement with experimental results for the family of SCFs.<sup>33,34</sup> The lowest-energy transitions, which are fingerprints of  $\text{Ti}_2\text{S}@D_{3h}\text{-C}_{78}(24109)$  due to the titanium-based character of the LUMO orbitals, are predicted at rather large wavelengths, in good agreement with the large spectral onset obtained from the experiments (1470 nm, see Table S2 in ESI). The feature-rich absorption region of  $\text{Ti}_2\text{S}@C_{78}$  at lower wavelengths, which resembles that of  $\text{Ti}_2\text{C}_2@D_{3h}\text{-C}_{78}$  and  $\text{Sc}_3\text{N}@D_{3h}\text{-C}_{78}$  and is due to cage-to-cage

transitions, is rather well reproduced at the TD-DFT level, both the position of the peaks as well as their relative intensities (see Figure S5 in ESI).

## Conclusion

In summary, a sulfide cluster metallofullerene containing only non-rare earth metals inside the cage,  $\text{Ti}_2\text{S}@D_{3h}\text{-C}_{78}(24109)$ , has been successfully synthesized using  $\text{SO}_2$  as a source in a Krätschmer-Huffman DC-arc reactor. The new clusterfullerene was characterized by mass spectrometry, UV-Vis-NIR absorption spectroscopy, cyclic voltammetry and DFT calculations. Based on the experimental and computational studies, the cage symmetry was unambiguously assigned to  $D_{3h}\text{-C}_{78}(24109)$ , the most stable cage for both empty  $\text{C}_{78}^{6-}$  and  $\text{Ti}_2\text{S}@C_{78}$ . The endohedral  $\text{Ti}_2\text{S}$  cluster has a nearly linear geometry and transfers six electrons to the  $\text{C}_{78}$  cage. Surprisingly,  $\text{Ti}_2\text{S}@D_{3h}\text{-C}_{78}(24109)$  exhibits both electrochemically reversible cathodic and anodic behavior, and a small electrochemical gap, which are remarkably different from those of the corresponding rare earth metallic cluster fullerenes.

## Acknowledgements

We thank the Robert A. Welch Foundation for an endowed chair, grant #AH-0033 and the US NSF for grant DMR-1205302, which provided generous support for this work. This work was also supported by the Spanish Ministry of Economy and Competitiveness (Project no. CTQ2011-29054-C02-01) and by the Generalitat de Catalunya (2009SGR462 and XRQTC). Additional support from the US NSF, grant CHE-1124075 and from the Spanish Ministry of Economy and Competitiveness (PRI-PIBUS-2011-0995) for a joint US-Spain collaboration is also acknowledged. M.M.-G. thanks the Spanish Ministry of Economy and Competitiveness for a doctoral fellowship.

**Electronic supplementary information (ESI) available:** Experimental sections and computational results.

## Notes and references

The calculations were conducted using DFT methodology with the ADF 2010 package.<sup>67</sup> The exchange-correlation functionals of Becke and Perdew were used.<sup>68,69</sup> Relativistic corrections were included by means of the ZORA formalism. Slater triple-zeta polarization basis sets were employed to describe the valence electrons of C, S and Ti. Frozen cores consisting of the 1s shell for C and the 1s and 2p shells for S and Ti were described by means of single Slater functions. The computational study of the UV-Vis-NIR spectra has been performed using TDDFT methodology (also at BP86/TZP level).

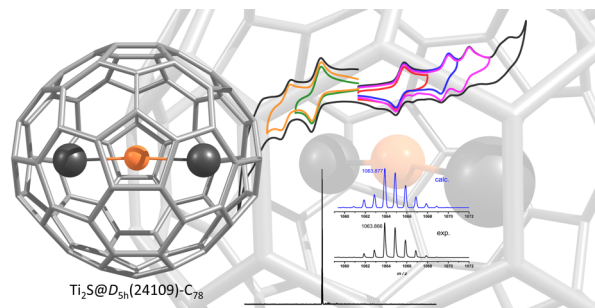
- 1 M. N. Chaur, F. Melin, A. L. Ortiz and L. Echegoyen, *Angew. Chem. Int. Ed.*, 2009, **48**, 7514-7538.
- 2 L. Dunsch and S. Yang, *Phys. Chem. Chem. Phys.*, 2007, **9**, 3067-3081.
- 3 S. Yang, F. Liu, C. Chen, M. Jiao and T. Wei, *Chem. Commun.*, 2011, **47**, 11822-11839.
- 4 L. Dunsch and S. Yang, *Small*, 2007, **3**, 1298-1320.
- 5 R. B. Ross, C. M. Cardona, D. M. Guldi, S. G. Sankaranarayanan, M. O. Reese, N. Kopidakis, J. Peet, B. Walker, G. C. Bazan, E. Van Keuren, B. C. Holloway and M. Drees, *Nat. Mater.*, 2009, **8**, 208-212.
- 6 J. R. Pinzón, M. E. Plonska-Brzezinska, C. M. Cardona, A. J. Athans, S. S. Gayathri, D. M. Guldi, M. Á. Herranz, N. Martín, T. Torres and L. Echegoyen, *Angew. Chem. Int. Ed.*, 2008, **47**, 4173-4176.
- 7 M. D. Shultz, J. C. Duchamp, J. D. Wilson, C.-Y. Shu, J. Ge, J. Zhang, H. W. Gibson, H. L. Fillmore, J. I. Hirsch, H. C. Dorn and P. P. Fatouros, *J. Am. Chem. Soc.*, 2010, **132**, 4980-4981.
- 8 E. B. Iezzi, J. C. Duchamp, K. R. Fletcher, T. E. Glass and H. C. Dorn, *Nano Lett.*, 2002, **2**, 1187-1190.
- 9 R. B. Ross, C. M. Cardona, F. B. Swain, D. M. Guldi, S. G. Sankaranarayanan, E. Van Keuren, B. C. Holloway and M. Drees, *Adv. Funct. Mater.*, 2009, **19**, 2332-2337.
- 10 C. Shu, W. Xu, C. Slebodnick, H. Champion, W. Fu, J. E. Reid, H. Azurmendi, C. Wang, K. Harich, H. C. Dorn and H. W. Gibson, *Org. Lett.*, 2009, **11**, 1753-1756.
- 11 C. Y. Shu, X. Y. Ma, J. F. Zhang, F. D. Corwin, J. H. Sim, E. Y. Zhang, H. C. Dorn, H. W. Gibson, P. P. Fatouros, C. R. Wang and X. H. Fang, *Bioconj. Chem.*, 2008, **19**, 651-655.
- 12 A. A. Popov and L. Dunsch, *Chem. Eur. J.*, 2009, **15**, 9707-9729.
- 13 A. Rodriguez-Forteza, A. L. Balch and J. M. Poblet, *Chem. Soc. Rev.*, 2011, **40**, 3551-3563.
- 14 M. Yamada, T. Akasaka and S. Nagase, *Acc. Chem. Res.*, 2009, **43**, 92-102.
- 15 A. A. Popov, S. M. Avdoshenko, A. M. Pendas and L. Dunsch, *Chem. Commun.*, 2012, **48**, 8031-8050.
- 16 S. Osuna, M. Swart and M. Sola, *Phys. Chem. Chem. Phys.*, 2011, **13**, 3585-3603.
- 17 X. Lu, T. Akasaka and S. Nagase, *Chem. Commun.*, 2011, **47**, 5942-5957.

- 18 S. Stevenson, G. Rice, T. Glass, K. Harich, F. Cromer, M. R. Jordan, J. Craft, E. Hadju, R. Bible, M. M. Olmstead, K. Maitra, A. J. Fisher, A. L. Balch and H. C. Dorn, *Nature*, 1999, **401**, 55-57.
- 19 S. Stevenson, P. W. Fowler, T. Heine, J. C. Duchamp, G. Rice, T. Glass, K. Harich, E. Hajdu, R. Bible and H. C. Dorn, *Nature*, 2000, **408**, 427-428.
- 20 C.-R. Wang, T. Kai, T. Tomiyama, T. Yoshida, Y. Kobayashi, E. Nishibori, M. Takata, M. Sakata and H. Shinohara, *Angew. Chem. Int. Ed.*, 2001, **40**, 397-399.
- 21 Z.-Q. Shi, X. Wu, C.-R. Wang, X. Lu and H. Shinohara, *Angew. Chem. Int. Ed.*, 2006, **45**, 2107-2111.
- 22 Y. Iiduka, T. Wakahara, T. Nakahodo, T. Tsuchiya, A. Sakuraba, Y. Maeda, T. Akasaka, K. Yoza, E. Horn, T. Kato, M. T. H. Liu, N. Mizorogi, K. Kobayashi and S. Nagase, *J. Am. Chem. Soc.*, 2005, **127**, 12500-12501.
- 23 H. Yang, C. Lu, Z. Liu, H. Jin, Y. Che, M. M. Olmstead and A. L. Balch, *J. Am. Chem. Soc.*, 2008, **130**, 17296-17300.
- 24 T.-S. Wang, N. Chen, J.-F. Xiang, B. Li, J.-Y. Wu, W. Xu, L. Jiang, K. Tan, C.-Y. Shu, X. Lu and C.-R. Wang, *J. Am. Chem. Soc.*, 2009, **131**, 16646-16647.
- 25 S. Stevenson, M. A. Mackey, M. A. Stuart, J. P. Phillips, M. L. Easterling, C. J. Chancellor, M. M. Olmstead and A. L. Balch, *J. Am. Chem. Soc.*, 2008, **130**, 11844-11845.
- 26 R. Valencia, A. Rodríguez-Forteza, S. Stevenson, A. L. Balch and J. M. Poblet, *Inorg. Chem.*, 2009, **48**, 5957-5961.
- 27 B. Q. Mercado, M. M. Olmstead, C. M. Beavers, M. L. Easterling, S. Stevenson, M. A. Mackey, C. E. Coumbe, J. D. Phillips, J. P. Phillips, J. M. Poblet and A. L. Balch, *Chem. Commun.*, 2010, **46**, 279-281.
- 28 T.-S. Wang, L. Feng, J.-Y. Wu, W. Xu, J.-F. Xiang, K. Tan, Y.-H. Ma, J.-P. Zheng, L. Jiang, X. Lu, C.-Y. Shu and C.-R. Wang, *J. Am. Chem. Soc.*, 2010, **132**, 16362-16364.
- 29 J. Wu, T. Wang, Y. Ma, L. Jiang, C. Shu and C. Wang, *J. Phys. Chem. C*, 2011, **115**, 23755-23759.
- 30 M. Krause, F. Ziegls, A. A. Popov and L. Dunsch, *ChemPhysChem*, 2007, **8**, 537-540.
- 31 L. Dunsch, S. Yang, L. Zhang, A. Svitova, S. Oswald and A. A. Popov, *J. Am. Chem. Soc.*, 2010, **132**, 5413-5421.
- 32 N. Chen, M. N. Chaur, C. Moore, J. R. Pinzon, R. Valencia, A. Rodríguez-Forteza, J. M. Poblet and L. Echegoyen, *Chem. Commun.*, 2010, **46**, 4818-4820.
- 33 N. Chen, C. M. Beavers, M. Mulet-Gas, A. Rodríguez-Forteza, E. J. Muñoz, Y.-Y. Li, M. M. Olmstead, A. L. Balch, J. M. Poblet and L. Echegoyen, *J. Am. Chem. Soc.*, 2012, **134**, 7851-7860.
- 34 N. Chen, M. Mulet-Gas, Y.-Y. Li, R. E. Stene, C. W. Atherton, A. Rodríguez-Forteza, J. M. Poblet and L. Echegoyen, *Chem. Sci.*, 2013, **4**, 180-186.
- 35 B. Q. Mercado, N. Chen, A. Rodríguez-Forteza, M. A. Mackey, S. Stevenson, L. Echegoyen, J. M. Poblet, M. M. Olmstead and A. L. Balch, *J. Am. Chem. Soc.*, 2011, **133**, 6752-6760.
- 36 L.-H. Gan, Q. Chang, C. Zhao and C.-R. Wang, *Chem. Phys. Lett.*, <http://dx.doi.org/10.1016/j.cplett.2013.03.067>.

- 37 T. Guo, M. D. Diener, Y. Chai, M. J. Alford, R. E. Haufler, S. M. McClure, T. Ohno, J. H. Weaver, G. E. Scuseria and R. E. Smalley, *Science*, 1992, **257**, 1661-1664.
- 38 B. I. Dunlap, O. D. Haerberlen and N. Roesch, *J. Phys. Chem.*, 1992, **96**, 9095-9097.
- 39 B. Cao, M. Hasegawa, K. Okada, T. Tomiyama, T. Okazaki, K. Suenaga and H. Shinohara, *J. Am. Chem. Soc.*, 2001, **123**, 9679-9680.
- 40 T. Yumura, Y. Sato, K. Suenaga and S. Iijima, *J. Phys. Chem. B*, 2005, **109**, 20251-20255.
- 41 K. Tan and X. Lu, *Chem. Commun.*, 2005, 4444-4446.
- 42 Y. Sato, T. Yumura, K. Suenaga, H. Moribe, D. Nishide, M. Ishida, H. Shinohara and S. Iijima, *Phys. Rev. B*, 2006, **73**, 193401.
- 43 B. Cao, K. Suenaga, T. Okazaki and H. Shinohara, *J. Phys. Chem. B*, 2002, **106**, 9295-9298.
- 44 S. Yang, C. Chen, A. A. Popov, W. Zhang, F. Liu and L. Dunsch, *Chem. Commun.*, 2009, 6391-6393.
- 45 C. Chen, F. Liu, S. Li, N. Wang, A. A. Popov, M. Jiao, T. Wei, Q. Li, L. Dunsch and S. Yang, *Inorg. Chem.*, 2012, **51**, 3039-3045.
- 46 P. W. Fowler and D. E. Manolopoulos, *An Atlas of Fullerenes*, Oxford University Press, Oxford, 1995.
- 47 H. Shinohara, *Rep. Prog. Phys.*, 2000, **63**, 843-892.
- 48 M. M. Olmstead, A. de Bettencourt-Dias, J. C. Duchamp, S. Stevenson, D. Marciu, H. C. Dorn and A. L. Balch, *Angew. Chem. Int. Ed.*, 2001, **40**, 1223-1225.
- 49 A. A. Popov, M. Krause, S. Yang, J. Wong and L. Dunsch, *J. Phys. Chem. B*, 2007, **111**, 3363-3369.
- 50 C. M. Beavers, M. N. Chaur, M. M. Olmstead, L. Echegoyen and A. L. Balch, *J. Am. Chem. Soc.*, 2009, **131**, 11519-11524.
- 51 J. M. Campanera, C. Bo and J. M. Poble, *Angew. Chem. Int. Ed.*, 2005, **44**, 7230-7233.
- 52 M. N. Chaur, R. Valencia, A. Rodriguez-Forte, J. M. Poble and L. Echegoyen, *Angew. Chem. Int. Ed.*, 2009, **48**, 1425-1428.
- 53 A. A. Popov, C. B. Chen, S. F. Yang, F. Lipps and L. Dunsch, *ACS Nano*, 2010, **4**, 4857-4871.
- 54 A. A. Popov, N. Chen, J. R. Pinzón, S. Stevenson, L. A. Echegoyen and L. Dunsch, *J. Am. Chem. Soc.*, 2012, **134**, 19607-19618.
- 55 T. Cai, L. Xu, C. Shu, H. A. Champion, J. E. Reid, C. Anklin, M. R. Anderson, H. W. Gibson and H. C. Dorn, *J. Am. Chem. Soc.*, 2008, **130**, 2136-2137.
- 56 B. Elliott, L. Yu and L. Echegoyen, *J. Am. Chem. Soc.*, 2005, **127**, 10885-10888.
- 57 M. Krause and L. Dunsch, *ChemPhysChem* 2004, **5**, 1445-1449.
- 58 C. M. Cardona, B. Elliott and L. Echegoyen, *J. Am. Chem. Soc.*, 2006, **128**, 6480-6485.
- 59 Y.-Z. Tan, S.-Y. Xie, R.-B. Huang and L.-S. Zheng, *Nat. Chem.*, 2009, **1**, 450-460.
- 60 A. Rodríguez-Forte, N. Alegret, A. L. Balch and J. M. Poble, *Nat. Chem.*, 2010, **2**, 955-961.
- 61 A. A. Popov, *J. Comput. Theor. Nanosci*, 2009, **6**, 292-317.

- 62 J. M. Campanera, C. Bo, M. M. Olmstead, A. L. Balch and J. M. Poblet, *J. Phys. Chem. A* 2002, **106**, 12356-12364.
- 63 T. Suzuki, Y. Maruyama, T. Kato, K. Kikuchi, Y. Nakao, Y. Achiba, K. Kobayashi and S. Nagase, *Angew. Chem. Int. Ed. Eng.*, 1995, **34**, 1094-1096.
- 64 M. Yamada, N. Mizorogi, T. Tsuchiya, T. Akasaka and S. Nagase, *Chem. Eur. J.*, 2009, **15**, 9486-9493.
- 65 Z. Slanina, S.-L. Lee, F. Uhlík, L. Adamowicz and S. Nagase, *Theor. Chem. Acc.*, 2007, **117**, 315-322.
- 66 Z. Slanina and S. Nagase, *ChemPhysChem*, 2005, **6**, 2060-2063.
- 67 G. te Velde, F. M. Bickelhaupt, E. J. Baerends, C. Fonseca Guerra, S. J. A. van Gisbergen, J. G. Snijders and T. Ziegler, *J. Comput. Chem.*, 2001, **22**, 931-967.
- 68 A. D. Becke, *Phys. Rev. A*, 1988, **38**, 3098-3100.
- 69 J. P. Perdew, *Phys. Rev. B*, 1986, **33**, 8822-8824.

## Table of Content



A sulfide cluster metallofullerene containing only non-rare earth metals inside the cage,  $\text{Ti}_2\text{S}@D_{3h}\text{-C}_{78}$ (24109) was synthesized. The endohedral  $\text{Ti}_2\text{S}$  cluster has a nearly linear geometry and transfers six electrons to the  $\text{C}_{78}$  cage.